Electronic Supplementary Material (ESI) for RSC Advances.

Supplementary Information

The F19W mutation reduces the binding affinity of the transmembrane $A\beta_{11-40}$ trimer to the membrane bilayer

Thanh Thuy Tran,[ab]* Feng Pan,[c] Linh Tran,[de] Christopher Roland[f] and Celeste Sagui[f]

[a]Laboratory of Theoretical and Computational Biophysics, Ton Duc Thang University, Ho Chi Minh City, Vietnam;

[b]Faculty of Applied Sciences, Ton Duc Thang University, Ho Chi Minh City, Vietnam.

[c]Department of Statistics, Florida State University, Tallahassee, Florida, USA

[d]Institute of Fundamental and Applied Sciences, Duy Tan University, Ho Chi Minh City, 700000, Vietnam

[e]Faculty of Natural Sciences, Duy Tan University, Da Nang City, 550000, Vietnam

[f]Department of Physics, North Carolina State University, Raleigh, North Carolina, USA

Email: tranthanhthuy@tdtu.edu.vn

Table S1: A summary of the mutation studies.

System/Sequence	Ref.	Type of Study	Mutation	Main Results
Trimer Aβ_{11-40}	28	REMD in water solution (AMBER force-field + TIP3P water)	Wild-type	β-content:42 $\pm$ 6 %, coil: 49 $\pm$ 7 %, Intermolecular interactions in the central hydrophobic cores stabilize the oligomer; Intermolecular polar contacts between D23 and residues 24-29 stabilize loop regions, Nter is maintain by intermolecular polar crossing contacts H13A-Q15B and H13B-Q15C.
Trimer Aβ_{11-40}	29	REMD in water solution (AMBER force-field + TIP3P water)	E22Q	The $\beta-$structure decreases in N-terminal but increases in C-terminal. The representative shapes of the E22Q trimer adopt a significant increase in $\beta-$structure (β : 47%). Enhancing the intramolecular polar contacts between the residue D23 to residues (24-29). The mutant is more stable than the WT.
Trimer Aβ_{11-40}	30	REMD in water (AMBER force-field + TIP3P water)	D23N	The D23N mutant has higher β-structure and stronger inter-chain interactions; There are structural changes, and the mutant has an enhanced aggregation rate. The Aβ fibril-binding ligands bind to the D23N and WT forms at different poses.
Trimer Aβ_{11-40}	31	REMD in water, (Amber99SB-ILDN, TIP3P water)	F19W	Secondary structure: 3% less β (39%) and 3% more coil content (52%) than WT; there is a decrease in most of the polar contacts, except for D23-K28 salt bridge (12%). Six mimima were identified in the free energy surface, which account for 20% of the total conformations. The binding free energy between neighbour chains of the mutant trimer increases by $\sim$ 28 kcal mol^{-1} but fluctuates significantly ($\pm$27.1 kcal mol^{-1}). The solvated F19W is more flexible than the WT in solution.
Trimer Aβ_{11-40}	32	REMD in DPPC lipid bilayer and in solution	E22K	The mutant size was larger than the WT; the β-content increases. Increasing contacts between peptide-membrane. The mutant is more stable than the WT.
Trimer Aβ_{11-40}	33	REMD in water + DPPC lipid bilayer	A21G	Conformational changes and wider free energy minima on the free energy surface and altered surface charges, weaker affinity to the DPPC lipid bilayers. These results are consistent with experimental data shown that A21G mutants of Aβ peptides have a lower aggregation rate.
Trimer Aβ_{11-40}	34	REMD in water + DPPC lipid bilayer	Wild-type	β: $\sim$ 40%, coil: 57%, salt-bridge D23-N27 stabilizes the loop region of the peptide. The trimer strongly attracts the DPPC lipid bilayer.

To be continued ...

System/Sequence	Ref.	Type of study	Mutation	Main results
$A\beta_{1-40}$	36	Experiment (Fluoresences)	F19W, F20W	F19W, F20W do not hinder fibril formation. Monomer F19W fluoresence displays remarkable blue-shift over monomer F20W. F20W has a less hydrophobic environment than F19W in Aβ fibrils.
Monomer $A\beta_{1-40}$	37	MD simulation in water	Double L17A/F19A	The β-sheet content decrease, the salt bridge D23-K28 decrease, the helical conformation is the dominant conformation in $A\beta_{40}$(L17A/F19A) L17A/F19A double mutation diminishes $A\beta_{40}$ aggregation.
Gene of the APP (Aβ-precusor protein)	38	Clinical experiments in the cerebral haemorrhage patients IV-3	A21G (Flemish)	Presenile dementia and cerebral haemorrhage linked to Flemish A21G mutant of the APP gene
Gene of the APP	39	Clinical experiments in the cerebral haemorrhage patients	Dutch D22Q	APP Gene and Hereditary Cerebral Hemorrhage with Amyloidosis (Dutch)
Gene of the Fatal familial insomnia (FFI)	40	Clinical experiments and genomic studies	Italian E22K	Fatal familial insomnia: Genetic, neuropathologic, and biochemical study of a patient from a new Italian kindred
$A\beta_{1-40}$ and $A\beta_{1-42}$	41	Discrete molecular dynamics (DMD) studies in implicit solvent	E22G	The average β-strand content in both alloforms increases with temperature. At physiological temperatures, both Aβ40 and Aβ42 adopt a collapsed-coil conformation with several short β-strands and a small (<1%) amount of α-helical structure. At slightly above physiological temperature, folded Aβ42 monomers display larger amounts of β-strands than the Aβ40 monomers. E22G disrupts contacts in the A21-A30 region of both mutant Aβ peptides, resulting in a less stable main folding region relative to the WT peptides. Artic mutant induces significant structural change at N-terminus of the Aβ40 peptide.
Monomer $A\beta_{1-40}$	42	MD simulation in water	E22G L17A/F19A/E22G	Increasing the helical content in the CHC and C-terminal region of [A17/A19/G22]Aβ40 as compared to [G22]Aβ40 [A17/A19/G22]Aβ40 reduces the fibril formation rate by 0.57 times of [G22]Aβ40 [A17/A19/G22]Aβ40 diminishes aggregation compared to [G22]Aβ40
Gene of the APP	43	Clinical experiments in the AD patients	E22Δ	There is mutant enhanced oligomerization but no fibrillization, as well as inhibited hippocampal long-term potentiation over the WT peptide in rats *in vivo*.
Gene of the APP	44	Clinical experiments in AD patients	D23N	Widespread neurofibrillary tangles, and unusually extensive distribution of Aβ40 in plaques. Increasing toxicity.
Monomer $A\beta_{42}$	45	REMD simulations	A2V	The β-sheet structure of A2V Aβ42 monomer is more than that in the wild-type monomer. A2V Aβ42 is more toxic than WT Aβ42.
$A\beta_{1-40}$	46	Experiments (fluorescence, transmission electron microscopy, X-ray diffraction, and solid-state NMR spectroscopy)	F19G, F19P, F19E, F19K, F19Y, F19W, L34E, and L34K	Local interactions impact the fibrillation kinetics, the structures (the intermolecular hydrogen bonds) and dynamics of the Aβ40, but leave the general fibril structure unchanged.
$A\beta_{1-40}$	47	Computational + experimental studies	F19K	The perturbation contacts K19-L34 influence the local structure of fibrils but eliminates cytotoxicity
Dimer $A\beta_{9-40}$ and dimer $A\beta_{9-42}$	48	MD in water (GROMOS96 ff + spc water)	A21G	The impact of the mutation A21G on Aβ structure and dynamics varies from Aβ40 to Aβ42. A21G destabilizes the β-sheets and in Aβ40, but not in Aβ42. Structural changes resulting in a reduced aggregation rate of Aβ fibrils containing the Flemish disease-causing mutation.
Present studies (F19W trimer $A\beta_{11-40}$)	this manuscript	REMD in water + DPPC lipid bilayer	F19W	The coil contents decrease $\sim$ 15.3% (average value 41.7%); the β-contents increases $\sim$ 4.46% (mean value 44.46%); essential salt-bridges (D23-N27 and D23-K28) disappear; total membrane-peptide contacts increases; structural diversity is greater with higher free energy values, the mutant is more flexible than the WT. Twelve minima were found in the free energy surface, with representative states in the form of two 3-stranded-β-sheets with either antiparallel or perpendicular patterns, which may act as nuleation for fibrillation. The binding free energy of protein-DPPC lipid bilayer increases by 46.74 kcal/mol.

Free Energy Perturbation (FEP) Method

In this method, the free energy difference between a system in its bound and unbound state is calculated as a function of a coupling parameter λ using MD simulations. Essentially, the bound state system is characterized with a Hamiltonian with λ set to zero, while the fully unbounded system is characterized by a Hamiltonian with λ equal to unity. Systems with intermediate values of λ are then defined such that the free energy change between neighbouring intermediate states with λ_i and λ_{i+1} is then $\Delta G_{\lambda_i \Rightarrow \lambda_{i+1}}$ which is calculated by means of Bennet's Acceptance Ratio (BAR)[1]. The full free energy difference between the unbound and the bound state is then obtained from a summation over all of these intermediate values:

$$\Delta G = \sum_{\lambda=0}^{\lambda=1} \Delta G_{\lambda_i \Rightarrow \lambda_{i+1}}$$

By varying λ from 0 to 1, the peptide is *de facto* annihilated from the transmembrane and solvated systems through an alteration of the non-bonded interactions, as illustrated in Figure S1. As a result, the peptide was annihilated twice in the two different systems; we therefore refer to the method as the double-annihilation binding free energy method.

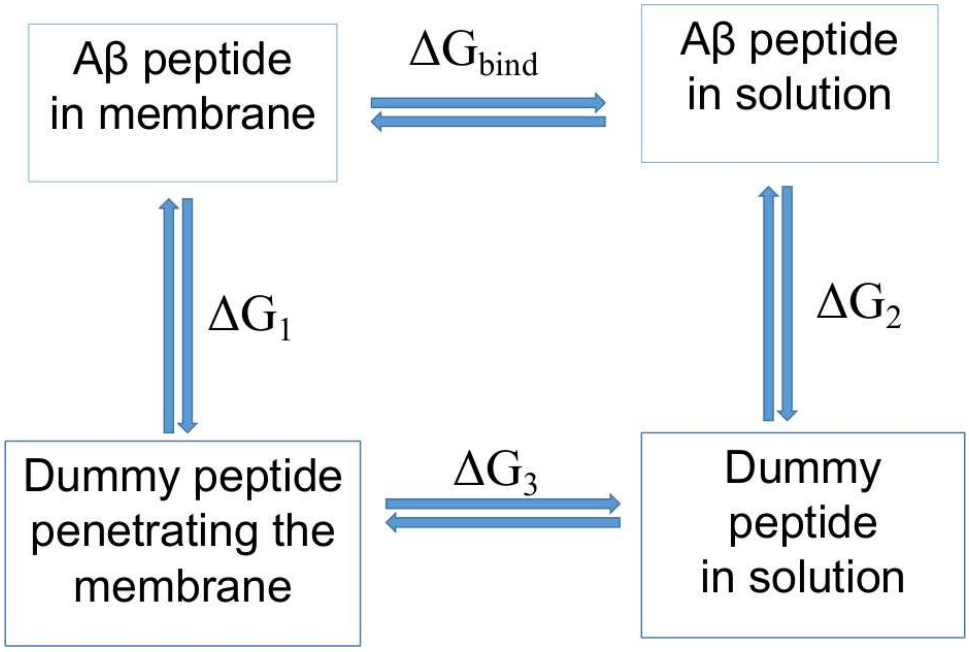

Figure S1: A schematic of the double-annihilation binding free energy method. In this scheme, Aβ peptide in the membrane represents the full-interaction state of the Aβ peptide with the solvated membrane system. Aβ peptide in solution represents the full-interaction state of the protein in solution, while the dummy protein indicates the protein without any interaction with surrounding molecules.

Our calculations here follow the previous work of Ngo et al.,[3]. A total of 15 values of λ were set up to reduce the non-bonded interactions from the full-interaction condition to the non-interaction mode with each simulation lasting 5 ns. The MD simulations were performed with the same starting conformations and initial velocities; but with different values of λ. The Coulomb interaction was reduced by six values of the coupling parameter λ, consisting of 0.00, 0.35, 0.55, 0.73, 0.88, and 1.00. The van der Waals interactions were set using 10 different λ values as follows: 0.00, 0.10, 0.20, 0.25, 0.30, 0.40, 0.55, 0.70, 0.85, and 1.00. Overall, the binding free energy of the truncated mutant trimer and the membrane lipid bilayers was given by:

$$\Delta G_{bind} = \Delta G_1 - \Delta G_2$$

Free Energy Surface (FES)

The FES of the mutant trimer was constructed using the "gmx sham" tools[4] of GROMACS with the root-mean-square deviation (RMSD) and the radius of gyration (Rg) serving as the reaction coordinates. The "gmx sham" creates a multi-dimensional free-energy by reading and analyzing data sets. It plots the Gibbs free energy landscapes by a Bolzmann invertion of the multi-dimensional histograms. In our study, a 2-dimensional FES was calculated using two reaction coordinates RMSD and Rg, with ranges 0.37 – 0.66 nm for RMSD, and 1.39 – 1.56 nm for Rg, respectively. The FES was calculated on a 40×40 grid.

Collision Cross Section (CCS)

The collision cross section (CCS) values of the F19W 3Aβ_{11-40} were calculated using The Ion Mobility Projection Approximation Calculation Tool (IMPACT)[2]. IMPACT can theoretically

calculate collision cross section of protein models through the projection approximation method. IMPACT can also estimate CCS values of proteins from their coordinate trajectory files produced from MD simulations, leading per-frame CCS measurements to be calculated in a high-throughput manner. Our calculations used IMPACT with the trajectory method.

References

[1] Bennett, C. H. Efficient estimation of free energy differences from monte carlo data. *J. Comput. Phys. 22* (1976), 245–268.

[2] Marklund, E. G., Degiacomi, M. T., Robinson, C. V., Baldwin, A. J., and Benesch, J. L. Collision cross sections for structural proteomics. *Structure 23*, 4 (2015), 791–799.

[3] Ngo, S. T., Hung, H. M., Tran, K. N., and Nguyen, M. T. Replica exchange molecular dynamics study of the amyloid beta (11-40) trimer penetrating a membrane. *RSC. Adv. 7*, 12 (2017), 7346–7357.

[4] Papaleo, E., Mereghetti, P., Fantucci, P., Grandori, R., and De Gioia, L. Free-energy landscape, principal component analysis, and structural clustering to identify representative conformations from molecular dynamics simulations: the myoglobin case. *J. Mol. Graph Model 27*, 8 (2009), 89–99.

The transmembrane mutant F19W $A\beta_{11-40}$ trimer was investigated using the temperature replica exchange molecular dynamics simulations with explicit solvent with 32 different replicas from 321 to 423 K. These temperatures are: 321.0, 323.9, 326.9, 329.9, 332.9, 335.9, 338.9, 342.0, 345.1, 348.2, 351.3, 354.5, 357.6, 360.8, 364.0, 367.3, 370.6, 373.9, 377.2, 380.5, 383.9, 387.3, 390.7, 394.1, 397.6, 401.1, 404.6, 408.1, 411.7, 415.3, 418.9, and 422.6 K.

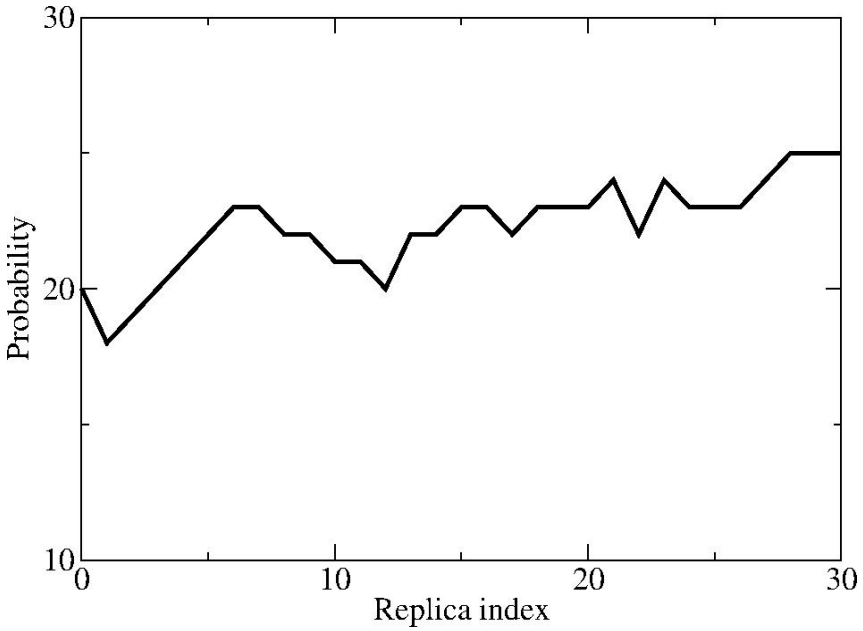

Figure S2: The mean exchange rates between neighboring replicas during 400 ns of REMD simulations.

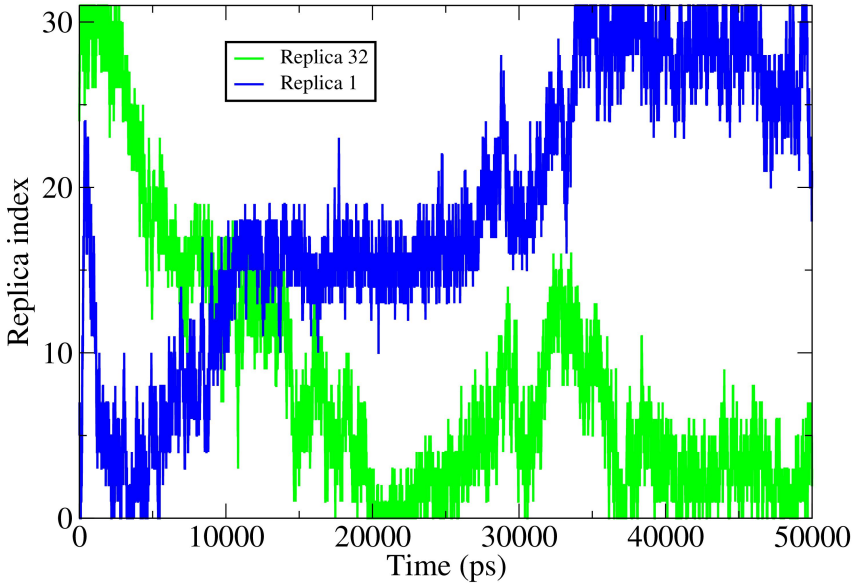

Figure S3. The temperature indices of replicas 1st and 32th are dispersed in the entire temperature space.

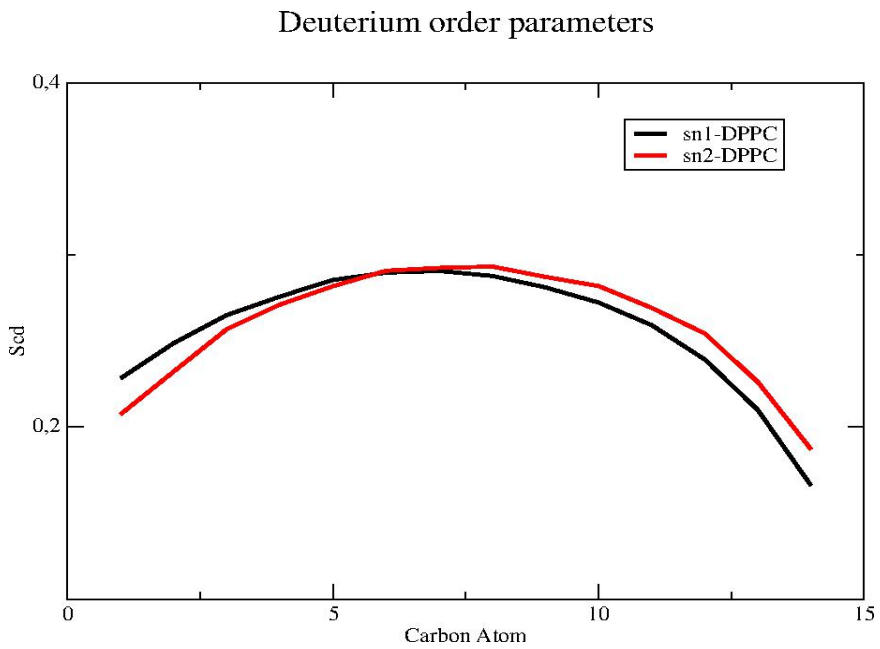

Figure S4. The lipid order parameters are investigated the both carbons atoms of acyl chains sn-1 (black) and sn-2 (red). The results are averaged over last 150 ns of the temperature REMD simulations.

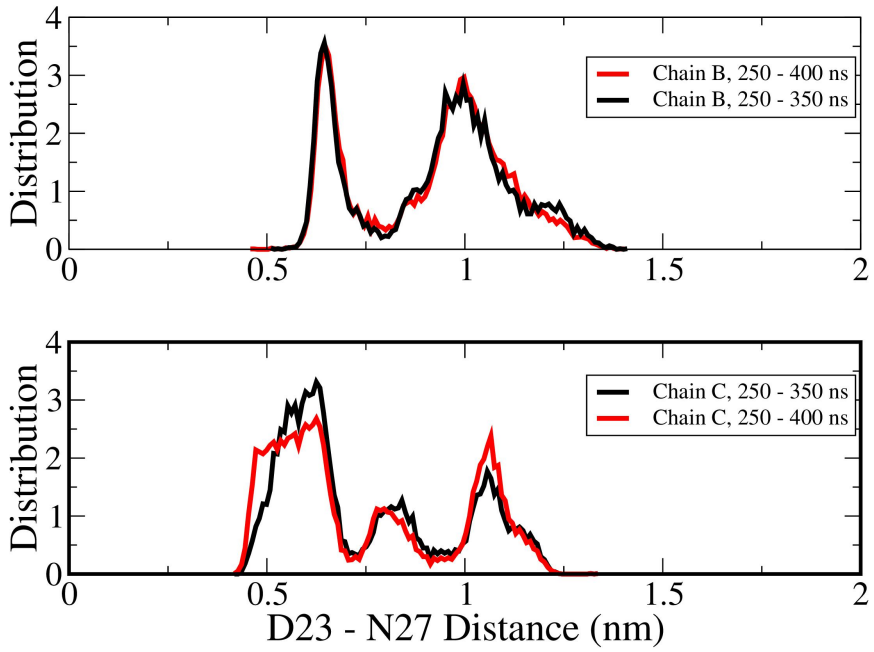

Figure S5. Convergence of REMD simulations at 324 K. Distance distributions between the charge groups of D23 and N27 of chain B and chain C of the transmembrane mutant F19W 3Aβ_{11-40}. The results were calculated for two time intervals 250-350 ns (black curves) and 250-400 ns (red curves).

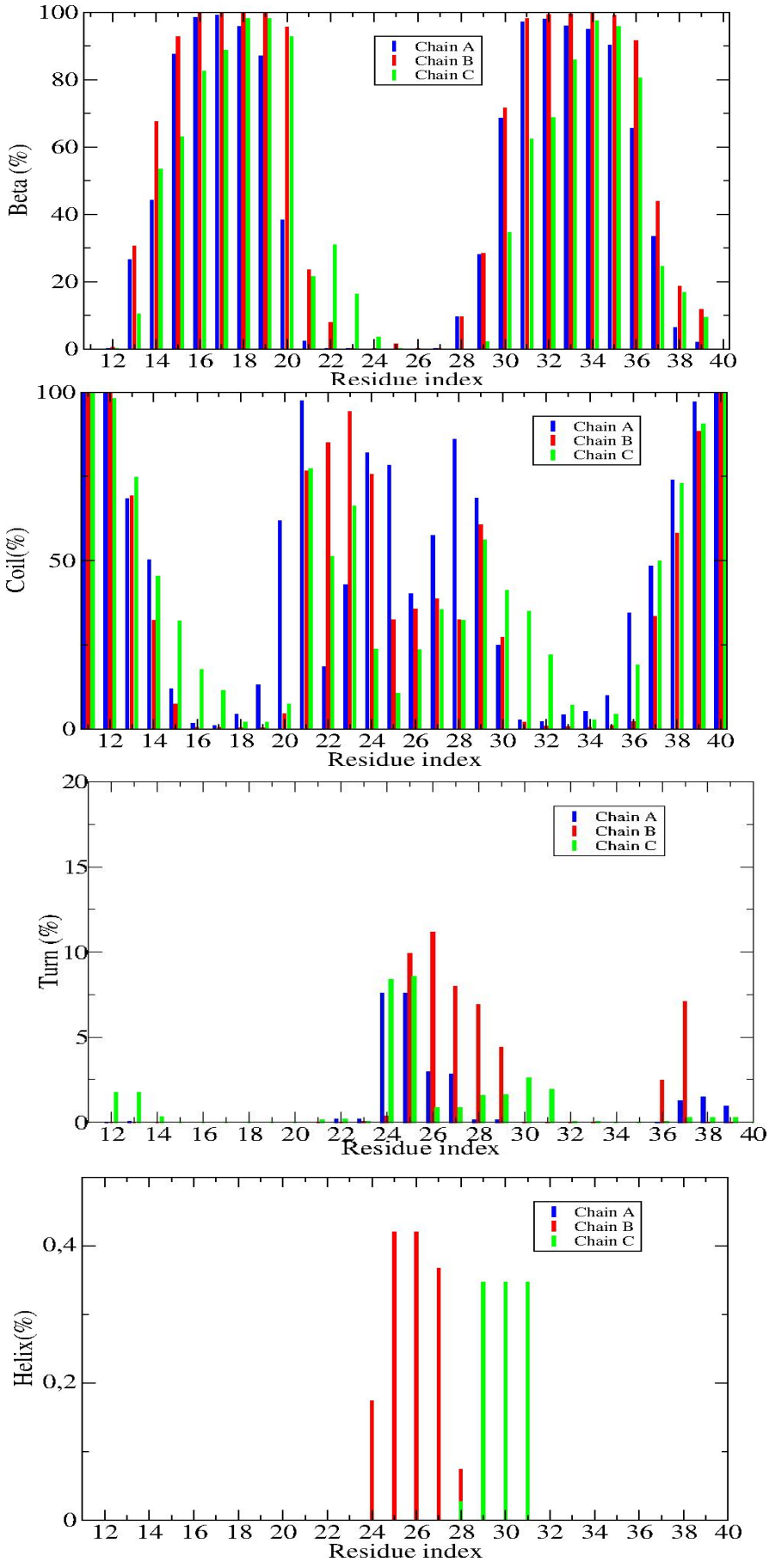

Figure S6. The secondary structure distribution per residue of transmembrane F19W 3Aβ_{11-40} peptide, which were averaged from the last 150 ns of REMD simulations at 324K using DSSP tools.

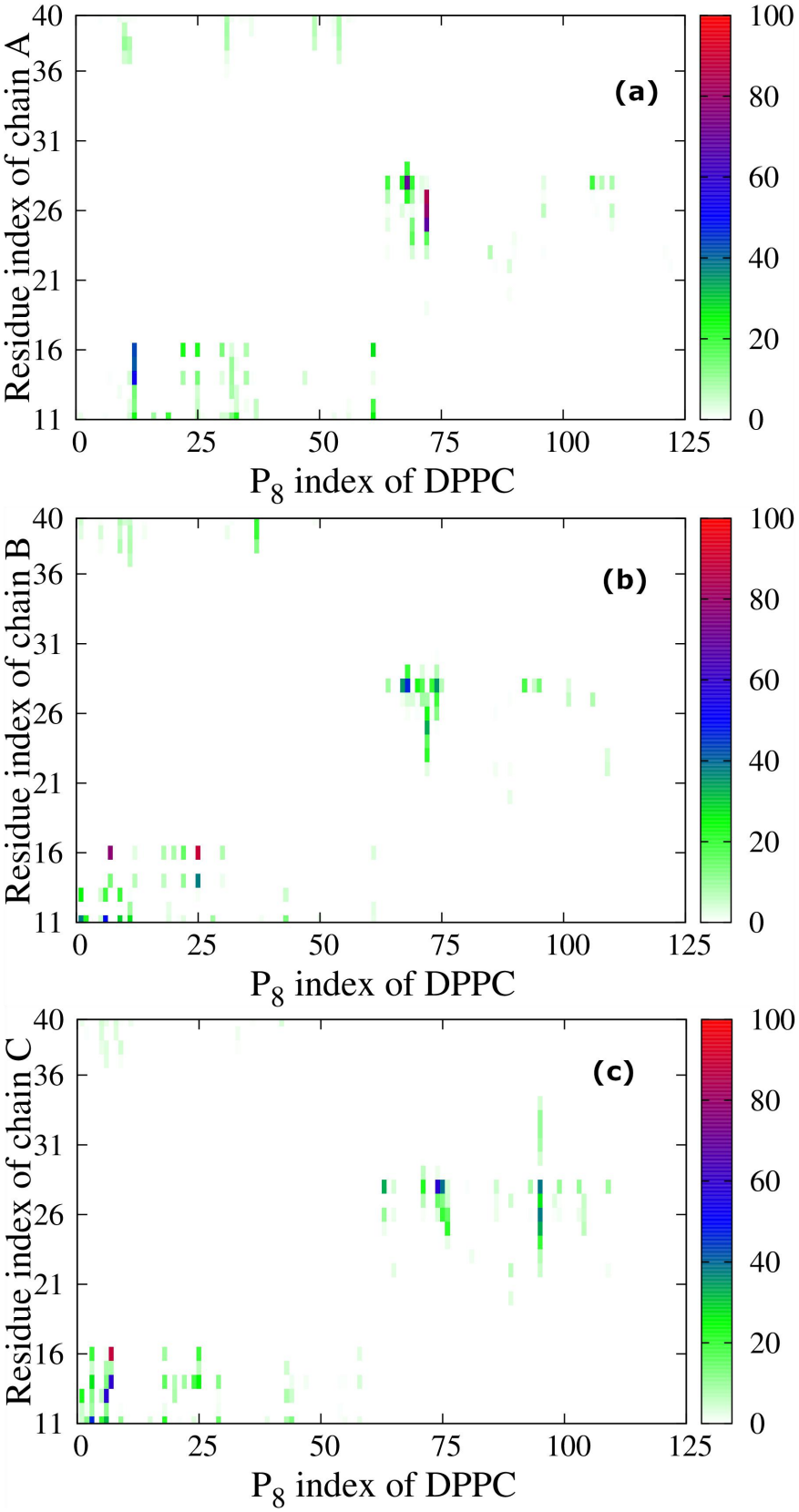

Figure S7: The contacts map between phosphate atom of lipid bilayers with each residues of each chain of the F19W 3Aβ$_{11-40}$

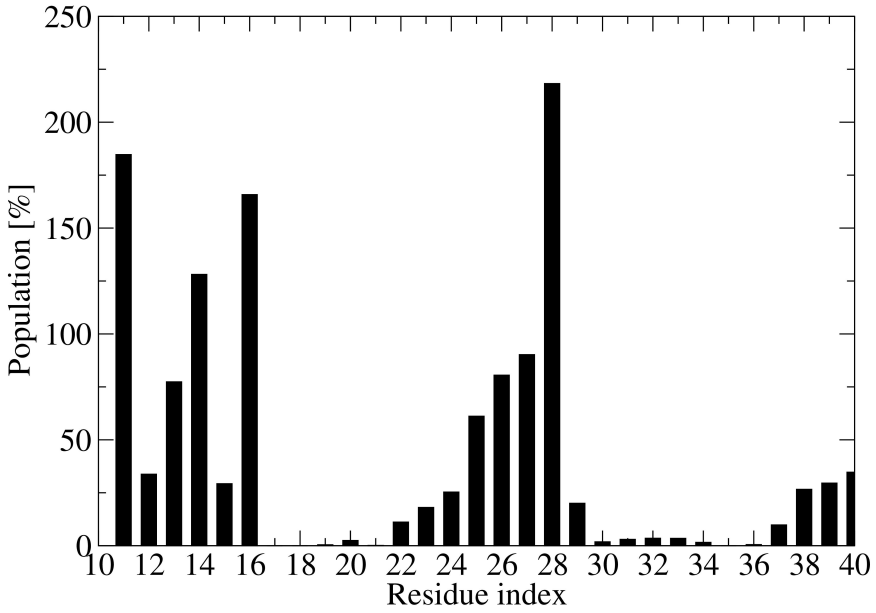

Figure S8: Averaged population of inter-molecular contacts between phosphate atoms of DPPC lipid bilayers and heavy atoms per residue of the truncated F19W $3A\beta_{11-40}$

Table S2: The probabilities of SC-SC inter-peptide contacts between neighbor pair chains of the truncated mutant trimer.

Probabilities	Chain A - Chain B (Figure 5a)	Chain B - Chain C (Figure 5b)
>80%	W19-W19 (97.44%), Q15-Q15 (93.81%), F20-F20 (93.41%), M35-M35 (92.10%), L17-L17 (88.47%), L34-L34 (86.17%)	F20-F20 (97.81%), L17-L17 (92.05%), W19-W19 (90.06%), L34-L34 (85.71%), M35-M35 (80.37%), Q15-H13 (80.31%)
60% - 80%	H14-H14 (79.92%), V18-F20 (79.65%), I31-I31 (75.65%), I32-I32 (75.16%) and V18-V18 (62.01%)	H13-H13 (77.61%), I32-I32 (73.42%), K16-K16 (72.67%), H14-H14 (66.79%), V18-V18 (66.32%), L34-W19 (64.78%), V36-L17 (61.65%), V18-F20 (60.57%) and V36-Q15 (60.42%)
40%-60%	**N-terminal – N-terminal:** K16-K16(52.04%),V12-H14(49.20%), H13-H13 (43.12%) **CHC – CHC:** A21-W19(56.30%),W19-L17(51.59%) **C-terminal – C-terminal:** I32-A30(50.71%), V36-V36 (49.76%) **C-terminal – CHC:** L34 – L17 (46.44%) **C-terminal – N-terminal:** V36-Q15 (56.22%)	V12-E11 (41.64%), A21-A21 (49.85%) L34-L17 (43.17%)

	Loop – Loop: N27-N27(46.58%), E22-E22 (41.82%)	
20%-40%	**N-terminal – N-terminal:** V12-V12(32.16%),V12-H13(33.69%), H14-H13(33.68%),Q15-H13(36.50%)**,** H13-E11(25.88%) **Loop – CHC:** E22-A21 (33.66%) **Loop – Loop:** E22-D23(30.17%);D23-N27 (27.04%), **C-terminal – C-terminal:** A30-A30 (21.78%), L34-I32(26.90%), V36-L34 (21.12%) **C-terminal – CHC:** V36-L17 (39.94%) **C-terminal – N-terminal:** V40-H13 (25.1%)	V12-V12(37.68%), V12-H14(36.90%) E22-E22 (29.11%) A30-A30 (24.34%) I32–A21 (30.89%), I32-W19 (28.42%), A30-A21 (23.91%) **CHC – CHC:** W19-L17(37.90%),A21-W19(35.83%) **C-terminal–loop:** A30 – D23: 22.91%
<20%	**C-terminal – C-terminal:** I32-L34(18.05%), L34-V36(17.48%), V36-V39(16.14%), V39- M35(11.57%), V40-V39(10.71%) **C-terminal – Loop:** A30-N27 (19.71%) **Loop – Loop:** K28-K28(19.74%), N27-S26(16.31%), N27-K28 (13.55%) **C-terminal – CHC:** I32-W19 (10.74%), L34-W19 (10.74%) **N-terminal – N-terminal:** V12-E11 (15.70%), H13-Q15 (12.27%), K16-H14 (14.55%) **N-terminal – CHC:**	I32-L34(12.88%), L34-V36(15.38%), V36-L34(19.72%), V40-V39(13.69%) I32- V24 (16.19%) L34-A21 (13.41%),V36-W19 (12.08%) V12-H13(15.51%), H13-E11 (11.41%),

	Q15-L17 (10%)	Q15-L17 (12.37%)

Table S3: The probabilities of BB-BB inter-peptide contacts between neighbor pair chains of the truncated mutant trimer.

Probabilities	Chain A - Chain B (Figure 5d)	Chain B - Chain C (Figure 5e)
>80%	I32-G33 (99.83%), L17-K16 (99.44%), L34-G33 (99.25%), L34-M35 (99.24%), K16-K16 (99.16%), I32-I31 (99.14%), L17-V18 (98.91%), Q15-K16 (98.77%), L17-L17 (97.89%), L34-L34 (97.58%), V18-V18 (97.52%), G33-G33 (96.97%), Q15-Q15 (96.56%), V30-I31 (96.11%), I32-I32 (95.37%), I31-I31 (95.18%), M35 - M35 (94.74%), V36-M35 (92.63%), Q15-H14(90.23%), W19-V18 (89.90%), W19-W19 (89.11%), A30-A30 (88.40%), V36 - V36 (88.05%) and W19-F20 (83.28%)	L34-M35 (99.45%), W19-W19 (98.40%), V18-V18 (98.09%), W19-F20 (98.06%), M35-M35 (97.93%), F20-F20 (97.77%), L17-V18 (97.33%), W19-V18 (95.81%), V36-M35 (94.83%), A21-F20 (94.55%), L17-L17 (94.25%), K16-K16 (93.89%), L34-L34 (93.85%), I32-G33 (93.71%), Q15-K16 (92.25%), L17-K16 (91.33%), L34-G33 (90.27%), G33-G33 (88.53%), V36-V36 (86.09%), V36-G37 (85.37%) and A21-A21 (83.31%).
60%-80%	H14-H14 (79.27%), F20-F20 (70.44%), V36-G37 (67.66%), G29-G29 (64.52%), G37-G37 (62.44%)	G37-G37 (77.45%), Q15-H14 (75.99%), Q15-Q15 (72.02%), H14-H14 (64.22%), I32-I32 (63.75%), I32-I31 (63.64%), H13-H14 (60.30%)
40%-60%	A21-F20 (55.24%), G29-K28 (40.48%), and H13-H14 (42.36%)	I31-I31 (59.93%) and A30-I31 (55.89%)
20%-40%	V38-V38 (39.94%), V38-V37 (39.64%), V30-G29 (39.84%), N27-N27 (23.86%), N27-S26 (20.77%), A21-A21 (22.75%), H13-H13 (31.59%), H13-V12 (26.38%) and V12 -V12 (25.82%)	residues 36 – 39 of chain B with residues 37 – 39 of chain C (mean probability of 27.59%) A30-A30 (35.17%), A30 with residues D23, V24 (38.33%), G29-A30 (20.55%), G29-D23 (23.18%), G29-V24 (31.91%), A21-E22 (35.84%), E22-E22 (22.30%) and H13 with residue E11, V12, H13 (probability of 27.65%)
<20%	K28-K28 (14.46%), N27-K28 (7.37%) and S26-S26 (7.29%)	A30-G25 (15%), G29-G25 (14.26%), G29-G29 (17%), G29-K28 (17%), K28-S26 (8.93%), D23-E22 (7.6%), D23-V24 (7.6%), N27-G25(7%).

Table S4: Characterizations of the structures of the first 4 main States S1-S4 of the transmebrane F19W 3Aβ_{11-40}: Shown are the β-strands and coils positions, the orientation of 2 β-sheets and the inter-peptide contacts that stabilize the 2 β-domains

State	**β-strands positions**	**Coils positions**	**Orientation of 2 β-sheets**	**Inter-peptide contacts**
S1	15-20, 28-36 : chain A 15-19, 28-36 : chain B 15-19, 28-35 : chain C	11-14, 21-27, 37-40: chain A 11-14, 20-27, 37-40: chain B 11-14, 20-27, 36-40: chain C	antiparallel	CHC-CHC, Cter-Cter and CHC-Cter, Nter-Nter between 2 adjacent pair chains
S2	14-23, 30-36 : chain A 14-21, 29-36 : chain B 15-20, 31-36 : chain C	11-13, 24-29, 37-40: chain A 11-13, 22-28, 37-40: chain B 11-14, 21-30, 37-40: chain C	perpendicular	Nter-Nter, CHC-CHC and Cter-Cter between 2 adjacent pair chains
S3	14-21, 31-35 : chain A 14-21, 30-36 : chain B 15-19, 30-36 : chain C	11-13, 22-30, 36-40: chain A 11-13, 22-29, 37-40: chain B 11-14, 20-29, 37-40: chain C	antiparallel	Nter-Nter, CHC-CHC and Cter-Cter
S4	16-22, 30-33 : chain A 15-22, 30-37 : chain B 15-17, 31-36 : chain C	11-15, 23-29, 34-40: chain A 11-14, 23-29, 38-40: chain B 11-14, 18-30, 37-40: chain C	antiparallel	CHC-CHC and Cter-Cter